



Published in final edited form as:

Physica E Low Dimens Syst Nanostruct. 2009 February ; 41(4): 723–728. doi:10.1016/j.physe.2008.11.018.

Preparation and characterization of sulfonic acid-functionalized single-walled carbon nanotubes

Luqman Adams^a, Aderemi Oki^{a,*}, Tony Grady^a, Hylton McWhinney^a, and Zhiping Luo^b

^a Department of Chemistry, Prairie View A&M University, Prairie View, TX 77446, USA

^b Microscopy and Imaging Center, Biological Sciences Building West 119, Texas A&M University, College Station, TX 77843-2257, USA

Abstract

A strategy for the functionalization of single-walled carbon nanotubes is reported. The synthesis involved the conversion of fluorinated single-walled carbon nanotubes to the thiolated derivative assisted by phosphorous pentasulfide. The thiol group is then quantitatively oxidized to the sulfonic acid group. The extent of oxidation of the thiol precursor is confirmed using X-ray photoelectron spectroscopy, which proved to be immensely useful to discriminate between the –SH and –SO₃H with a chemical shift for the sulfur 2p (approx. 5 eV). The functionalized carbon nanotubes were further characterized by infrared spectroscopy, thermogravimetric analysis, and transmission electron microscopy which revealed a significant change in morphology between the fluoro carbon nanotubes, the thiol and sulfonic acid-modified carbon nanotubes.

Keywords

Carbon nanotubes; Sulfonic acid

1. Introduction

The extraordinary properties of carbon nanotubes [1–5] and the vast areas of potential applications, in medicine, based on their ability to interact with biomolecules, such as proteins and oligosaccharides [6,7], as scanning microscope probe tip [8], as hydrogen storage materials [9], as fillers for ultra-high strength composites [10], and as electron field emitters [11] are some of potential areas of applications under exploration. In order to fully realize potential applications of carbon nanotubes in these and other areas, modification of the surfaces either by molecular self-assembly or chemical functionalization is usually required [12–14]. The covalent functionalization appears to offer strategic advantages over noncovalent approaches, such as polymer wrapping [15], biomolecule binding [16], and metal ion binding [17]. The improvement in solubility and better control of the surface chemistry to impart new characteristics on nanoscale materials are easily accomplished through covalent functionalization of carbon nanotubes [18].

Thiol-functionalized multi-wall carbon nanotubes (MWCNTs) have been prepared by exposing the MWCNTs to harsh acid treatment, which induced surface defect sites such as hydroxyl and carboxyl groups that are further reacted with P₄S₁₀ to afford reaction products such as MWCNT-SH, -CSOH, and -CSSH [19]. Other methods reported in the literature includes modification of surface oxidized groups with SOCl₂ and subsequent reaction with

*Corresponding author. Tel.: +19362613105; fax: +19362613117. aroki@pvamu.edu (A. Oki).

2-mercapto ethylbromide [20], or introduction of surface oxidized groups by mechano-chemical modification followed by reaction with H_2S [21]. Single-walled carbon nanotubes were oxidized and thiolated by means of amidation reaction activated by SOCl_2 [22], or converted to the sulfonic acid derivative by the hydrothermal method [23].

In this paper, we report a strategy that does not entail an initial surface oxidation protocol with neither an acid, nor a mechano-chemical approach to single-walled carbon nanotubes functionalized with thiol and sulfonic acid groups. This simple and efficient surface-substitution approach furnishes sulfur containing functionality covalently bonded to the surface of single-walled carbon nanotubes that is set up for other practical applications.

2. Experimental

The fluorinated single-walled carbon nanotubes (CNT-F) produced by the elemental fluorine method was provided by Dr. Valery Khabashesku (RICE University). The CNT-F was used as received after characterization by elemental analysis and thermogravimetric analysis. The elemental analysis shows a C_4F , formula. The following commercially available reagents P_4S_{10} , ethanol, sodium metal, sulfuric acid 98%, and HPLC grade isopropyl alcohol were obtained from Sigma-Aldrich, while hydrogen peroxide 30% (H_2O_2) obtained from Mallinckrodt was used in this research.

Fourier transform infrared spectroscopy (FTIR, IR-200 Thermo-Nicolet 2.2) (KBr) in the range $400\text{--}4000\text{ cm}^{-1}$ was used to confirm the covalently bound thiol and sulfonic acid groups on the CNT surface. Transmission electron microscopy (TEM) with a conventional 15 kV electron microscope was used to analyze the surface morphology of the functionalized carbon nanotubes. The thermal gravimetric analysis was performed under nitrogen on approximately 10 mg samples on a Universal V3.4C TA instruments. The run consisted of a ramp at a steady rate of $10\text{ }^\circ\text{C}/\text{min}$ from 40 to $800\text{ }^\circ\text{C}$ in air. The X-ray photoelectron spectroscopy (XPS) powder samples were collected with a Perkin Elmer PHI 5600 XPS for the surface analysis using the Mg $K\alpha$ X-ray line of 1253.6 eV excitation energy, 300 W, 15 kV. The vacuum base pressure was approximately 1×10^{-8} Torr. The adventitious carbon 284.6 eV binding energy line was used as an internal standard. Spectrometer pass energy of 58.7 eV was utilized. Carbon nanotube samples were set on indium foil, and then placed on the sample holder for analysis in the XPS surveys and multiplex. Carbon, oxygen, sodium, fluorine and sulfur analysis were carried out on each sample. An electron flood gun was used to minimize any charging effects during analysis.

In a typical experiment, 70.0 mg of P_4S_{10} was stirred for 15 min in a previously prepared solution of sodium 60.0 mg/ethanol 7 ml to generate hydrogen sulfide which undergoes further reaction with the sodium ethoxide to produce soluble sodium hydrogen sulfide in the suspension [24]. To this suspension 22 mg of fluoro carbon nanotubes (CNT-F) was added and heated at $70\text{ }^\circ\text{C}$ for 3 h. The black residue obtained after filtration with a $0.2\text{ }\mu\text{m}$ membrane was washed with three portions of 10 ml ethanol and dried under vacuum to afford the sidewall thiolated carbon nanotubes, CNT-SH, **1**. Thereafter, the sulfonic acid-functionalized carbon nanotube was prepared by oxidation of **1** obtained with 30% H_2O_2 (5.0 ml) at $60\text{ }^\circ\text{C}$ for 1 h [25]. The product obtained was filtered through a $0.2\text{ }\mu\text{m}$ membrane, washed with ethanol and re-suspended with stirring in 10% H_2SO_4 (10.0 ml) for 1 h to ensure complete protonation. The oxidation product after filtering through a $0.2\text{ }\mu\text{m}$ membrane was washed with deionized water until neutral pH and dried at $80\text{ }^\circ\text{C}$ for 12 h to give **2**.

Control experiments were designed as follows: (i) 10.0 mg of CNT-F was stirred with 10% H_2SO_4 (10.0 ml) for 1 h at ambient temperature. The work-up was performed as for **2** above

and (ii) 10.0 mg of CNT-F was reacted with 30% H₂O₂ (5.0 ml) at 60 °C for 1 h. The product was filtered through a 0.2 μm membrane and dried at 80 °C for 12 h.

3. Results and discussion

The thiol **1**, and sulfonic acid **2**, functionalized CNT were prepared according to the strategy described in Scheme 1.

XPS analysis was performed on pristine CNT, and the following derivatives: CNT-F, CNT-SH, and CNT-SO₃H with the aim of obtaining information on the functional groups on the carbon nanotube surface (Fig. 1(a-d)). XPS data for the control experiments (Fig. 5(a) and (b)) were also analyzed.

The X-ray photoelectron spectrum in the carbon 1s region is shown in Fig. 1(a). The main peaks appear at 284.6 eV with a non-symmetrical edge at the higher binding energy side of the peak. This has been generally referred as the sp² C=C/sp³ C-C bonding [26]. The pristine CNT shows a peak at ~291 eV. This is typical of the position for carbon π-π* shake up satellite peak of the sp²-hybridized carbon atoms which is more prominent in CNT-SH, **1** compared to the CNT-SO₃H, **2** functionalized carbon nanotube. The peak at ~288.5 eV confirms the C-F bond [26].

In Fig. 1(b), the fluorine 1s region further distinguishes the C-F bond of the CNT-F from the pristine CNT. The absorption peak in this region for the CNT-SH, **1** shows a strong band at ~685.2 eV associated with sodium (NaF) [27] byproduct distinguishable from the CNT-F at ~687.2 eV [26], which is further evidence for sidewall fluoro group displacement. The F 1s XPS spectra for **1** and **2**, functionalized CNT shows very weak peaks centered at ~687 eV suggesting only trace amounts of starting CNT-F compound particularly in the product CNT-SH, **1**.

In Fig. 1(c), the bands in the sulfur 2p region as expected indicate no sulfur moiety for the CNT and CNT-F compounds. Interestingly, the CNT-SH shows two separate peaks centered at ~163.5 and ~169.5 eV. The peak at 169.5 eV is assigned to a higher oxidation state of sulfur, CNT-SO₃H, **2** [25], while the peak at 163.5 eV shows a reduced form of sulfur as in a mercaptan, CNT-SH, **1** [21,25].

The oxygen 1s region, Fig. 1(d), shows that all the peaks occur between 535 and 530 eV with peak maxima at ~532.5 eV. The interpretation suggests that the oxygen is in the -2 oxidation state for the entire specimen.

Thermal degradation of the samples was monitored with TGA as shown in Fig. 2(a) and (b). The CNT-SH, **1** analysis, Fig. 2(a), display a gradual trend in decomposition from 40 to 430 °C with a weight loss of about 20%, probably coming from the loss of the adsorbed volatiles on the functionalized carbon nanotubes. This is followed by a sharp weight loss between 430 and 480 °C probably due to the loss of the covalently bonded thiol side group on the CNT framework with a weight loss of about 28%. In the CNT-SO₃H, **2** analysis, Fig. 2(b), a gradual trend in weight loss from 40 to 300 °C, arising from adsorbed volatiles molecules on the carbon nanotubes. This is followed by another weight loss between 300 and 560 °C due to decomposition of covalently bonded SO₃H side groups on the carbon nanotubes. The SO₃H may have further decomposed to release oxygen to the environment which ultimately led to sharp increase in weight loss between 560 and 640 °C attributed to the CNT framework decomposition in the presumably oxygen-rich nitrogen atmosphere.

Infrared spectroscopy analysis, Fig. 3(a) and (b), shows a mode centered at about 1540 cm⁻¹ assigned to stretching mode of the C=C double bond that forms the framework of the carbon

nanotubes sidewall. Fig. 3(a) shows characteristic modes centered at about 700 and 1145 cm^{-1} for the $-\text{SH}$ group in **1**, while the $-\text{SO}_3\text{H}$ group in **2**, Fig. 3(b) is shown by the band centered at 1202 cm^{-1} . The broad absorptions centered between 3000 and 3500 cm^{-1} may also be attributed partly to adsorbed solvents.

TEM analysis assists with direct imaging of the sidewall modification of the CNT-F. Fig. 4(a–c) shows the TEM images of the CNT-F, CNT-SH, and CNT-SO₃H, respectively, placed on carbon-coated copper grid. In all three functionalized single-walled carbon nanotubes, the TEM images show evidence of small kinks on the sidewalls, which appears more pronounced in the thiolated CNT (<0.5 nm). In addition, the CNT-SH **1** carbon nanotubes also appears to be aligned together probably through the thiol groups. This alignment appears disrupted when $-\text{SH}$ in **1** is oxidized to the $-\text{SO}_3\text{H}$ group in **2**.

Control experiments of CNT-F with 10% H_2SO_4 and 30% H_2O_2 , respectively, were performed to elucidate if the former mild acid medium can introduce on the CNT surface SO_3H groups, while the later is to investigate the fate of the fluoro substituent in the event of successful sulfonation under the mild acid control conditions. The carbon 1s region in Fig. 5(a) shows a band centered at about 288.5 eV for the starting CNT-F (similar to Fig. 1(a)) suggesting that under the control experimental conditions the fluoro group is not displaced. Furthermore, sulfur 2p region in the control, Fig. 5(b), does not show evidence of introduction of sulfur-related peaks under the mild 10% H_2SO_4 conditions. Although there is an apparent offset in the maxima of the binding energy between **1** and **2** in Fig. 1(c), the peaks are however centered at about the same point seen also in Fig. 5(b).

4. Conclusions

A route utilizing milder conditions starting from CNT-F offers the opportunity for substitution with other groups. XPS analysis is highly informative in tracking the surface chemistry occurring in these reactions, and has assisted with assignment of the $-\text{SH}$ and $-\text{SO}_3\text{H}$ peaks [21,25]. The result of this study suggests that the NaSH generated *in situ* can be used to introduce a thiol group by displacement of fluoro group on carbon nanotubes. Of significance is the alignment of thiolated CNT-SH as seen from the TEM in Fig. 5(b) which also suggests the potential and possibility of exploiting such surface to deposit proteins, enzymes, and other biomolecules.

Acknowledgments

The PIs acknowledge the support from NIH-NIAMSD Grant #ARO49172, NIH-NIGMS RISE Grant #1 R25 GM078361-01, the Welch Foundation and the US Air Force Research Laboratory-Minority Leaders Nanocomposite project.

References

1. Iijima S. Nature 1991;354:56.
2. Wildoer JWG, Venema L, Rinzler A, Smalley R, Dekker C. Nature 1998;391:59.
3. Odom TW, Huang TJL, Kim P, Lieber C. Nature 1998;391:62.
4. Qian D, Wagner GJ, Liu WK, Yu MF, Ruoff RS. Appl. Mech. Rev 2002;55:495.
5. Chen Y, Haddon RC, Fang S, Rao AM, Eklund PC, Lee WH, Dickey EC, Grulke EA, Pendergrass JC, Chaven A, Haley BE, Smalley RE. J. Mater. Res 1998;13:2423.
6. Belavoine F, Schultz P, Richard C, Mallouh V, Ebbesen TW, Mioskowski C. Angew. Chem. Int. Ed 1999;38:1912.
7. Chen RJ, Zhang Y, Wang D, Dai H. J. Am. Chem. Soc 2001;123:3838. [PubMed: 11457124]
8. Wong S, Woolley A, Joselevich E, Lieber C. Chem. Phys. Lett 1999;306:219.

9. Hirscher M, Becher M. J. *Nanosci. Nanotechnol* 2003;3:3. [PubMed: 12908227]
10. Rege K, Ravivakar NR, Kim DY, Schadler LS, Ajayan PM, Dordick JS. *Nano Lett* 2003;3:829.
11. De Heer WA, Chatelain A, Ugarte D. *Science* 1995;270:1179.
12. Bahr JL, Yang Y, Kosynkin DV, Bronikowski MJ, Smalley RE, Tour JM. *J. Am. Chem. Soc* 2001;123:6536. [PubMed: 11439040]
13. Star A, Stoddart JF, Steuerman D, Diehl M, Boukai A, Wong EW, Yang X, Chung S, Choi H, Heath JR. *Angew. Chem* 2001;40:1721. [PubMed: 11353491]
14. Haremza JM, Hahn MA, Krauss TD. *Nano Lett* 2002;2:1253.
15. Curran SA, Ajayan PM, Blau WJ, Carroll DL, Coleman JN, Dalton AB, Davey AP, Drury A, McCarthy B, Maier S, Strevens A. *Adv. Mater* 1998;10:1091.
16. Balavoine F, Schultz P, Richard C, Mallouh V, Ebbesen TW, Mioskowski C. *Angew. Chem. Int. Ed* 1999;38:1912.
17. Bond AM, Miao W, Raston CC. *Langmuir* 2000;16:6004.
18. Chen J, Hamon MA, Hu H, Chen Y, Rao AM, Eklund PC, Haddon RC. *Science* 1998;282:95. [PubMed: 9756485]
19. Cech J, Curran SA, Zhang D, Dewald JL, Avadhanula A, Kandadai M, Roth S. *Phys. Status Solidi (b)* 2006;243:3221.
20. Hu J, Shi J, Li S, Qin Y, Guo ZX, Song Y, Zhu D. *Chem. Phys. Lett* 2005;401:352.
21. Konya Z, Vesselenyi I, Niesz K, Kukovecz A, Demortier A, Fonseca A, Delhalle J, Mekhalif Z, Nahy JB, Koos AA, Osvath Z, Kocsonya A, Biro LP, Kiricsi I. *Chem. Phys. Lett* 2002;360:429.
22. Liu J, Rinzle AG, Dai H, Hafner JH, Bradley RK, Boul PJ, Lu A, Iverson T, Shelimov K, Huffman CB, Rodriguez-Macias F, Shon YS, Lee TR, Colbert DT, Smalley RE. *Science* 1998;80:1253. [PubMed: 9596576]
23. Duesberg GS, Graupner R, Downes P, Minett A, Ley L, Roth S, Nicoloso N. *Synth. Metal* 2004;142:263.
24. Eibeck RI. *Inorg. Synth* 1963;7:128.
25. Cano-Serrano E, Blanco-Brieva G, Campos-Martin JM, Fierro JIG. *Langmuir* 2003;19:7621.
26. Okpalugo TIT, Papakonstantinou P, Murphy H, McLaughlin J, Brown NMD. *Carbon* 2005;43:153.
27. Moulder, JF.; Stickle, WF.; Sobol, PE.; Bomben, KD. *Handbook of Standard Spectra for Identification and Interpretation of XPS Data*. Chastain, J., editor. Perkin-Elmer Corporation; USA: 1992. p. 51-52.

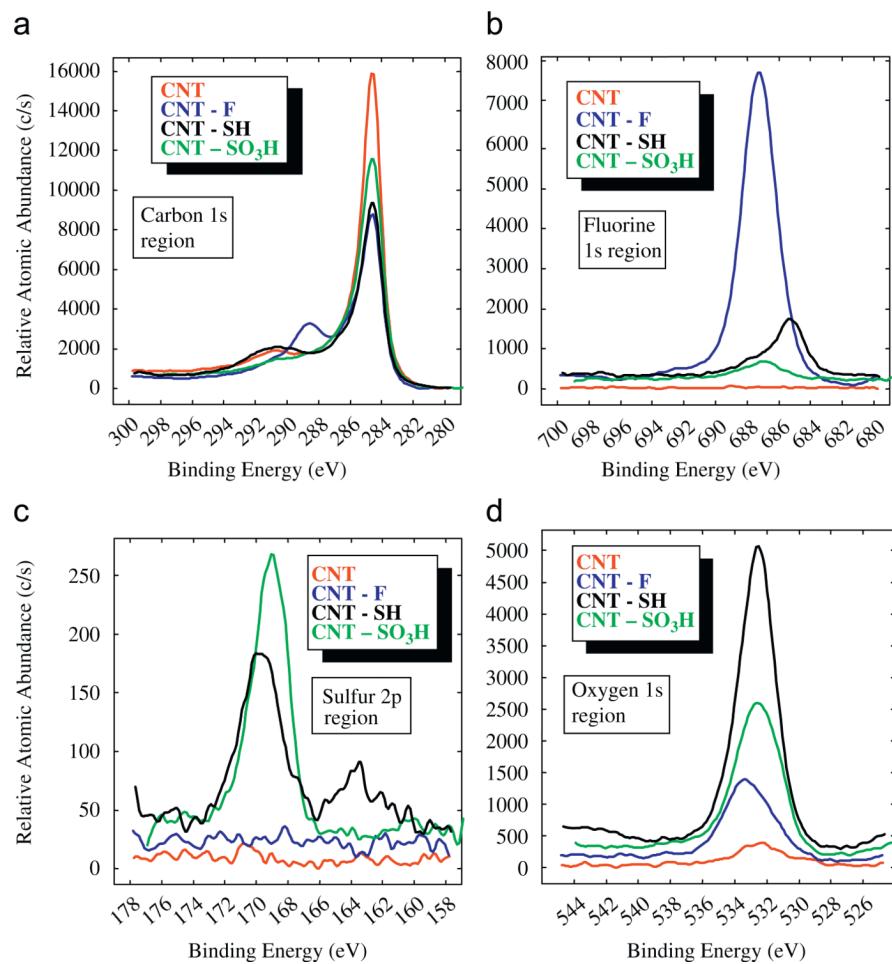


Fig. 1. XPS spectra in the regions of (a) C 1s, (b) F 1s, (c) S 2p, and (d) O 1s for SWCNT, CNT-F, CNT-SH, and CNT-SO₃H.

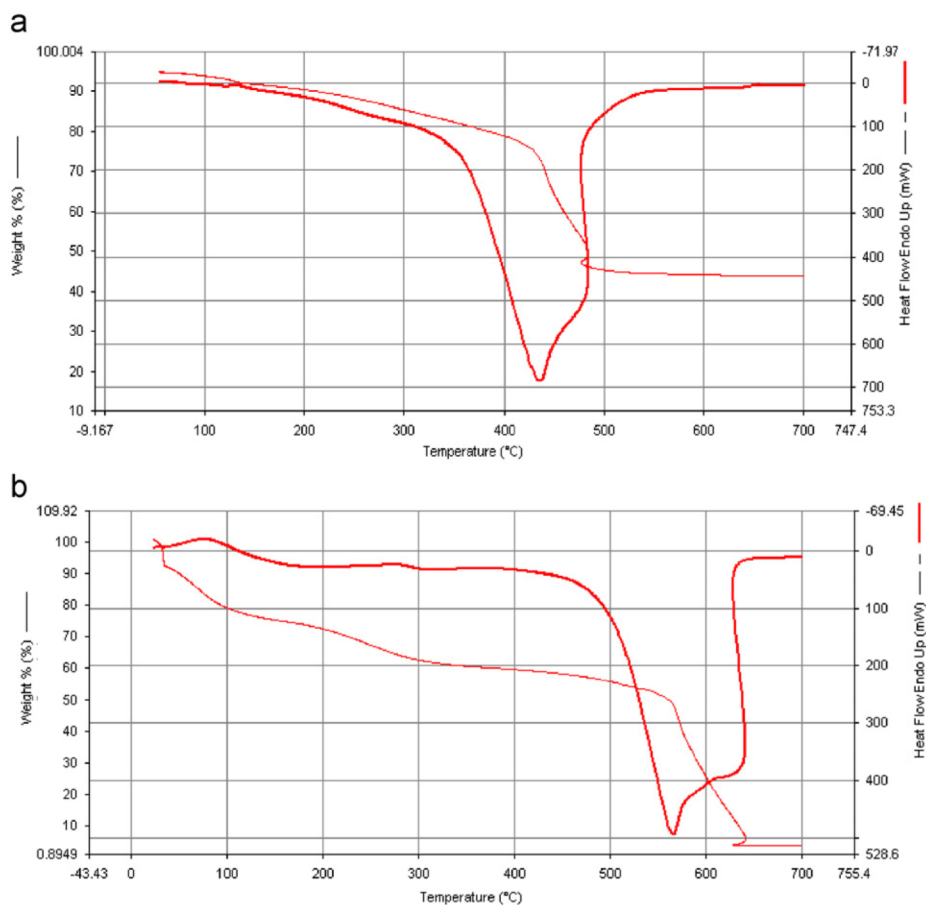


Fig. 2. TGA analysis for (a) CNT-SH and (b) CNT-SO₃H.

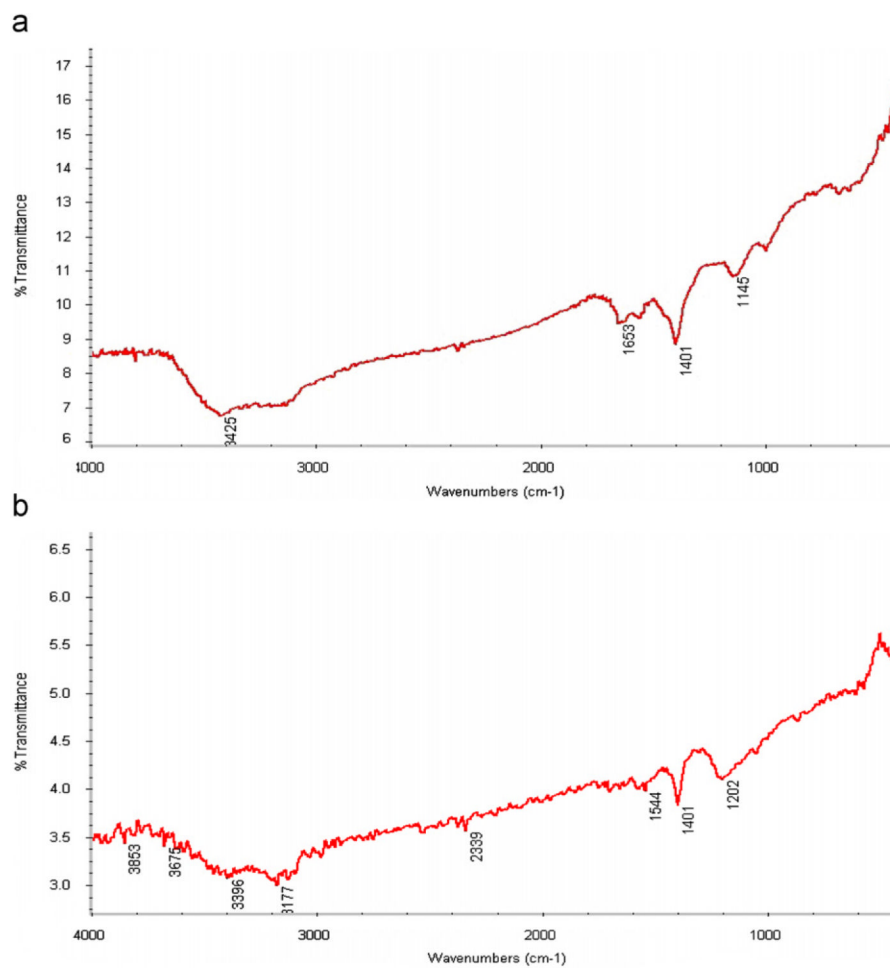


Fig. 3. FTIR analysis for sulfur-functionalized nanotubes (a) CNT-SH, 1 and (b) CNT-SO₃H, 2.

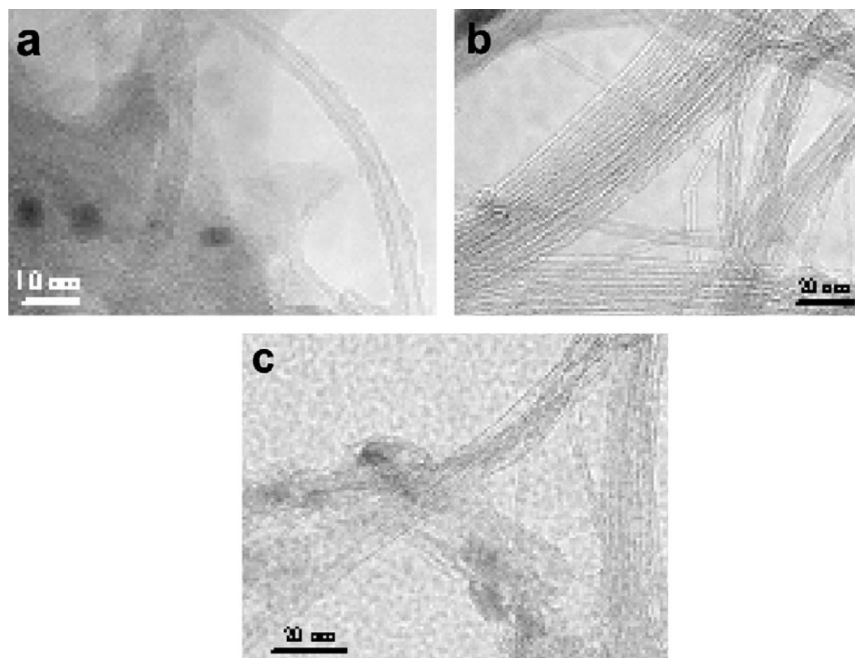


Fig. 4. TEM images of (a) CNT-F, (b) CNT-SH, and (c) CNT-SO₃H.

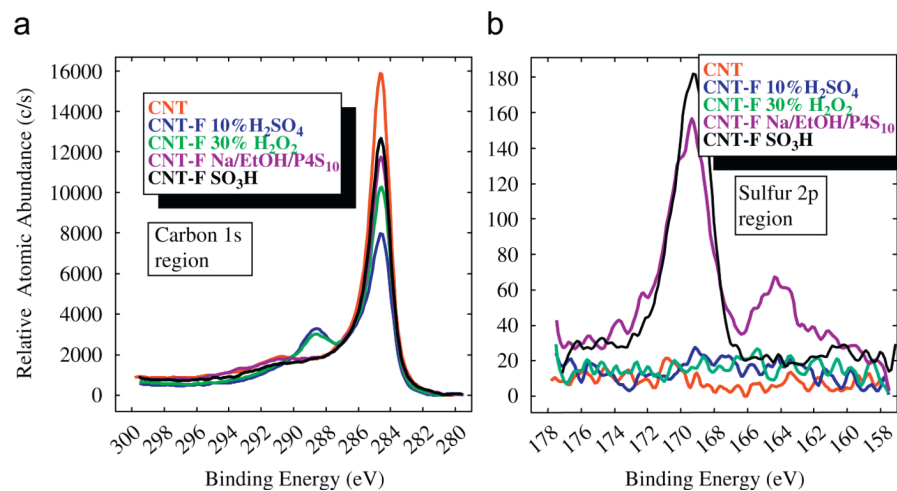
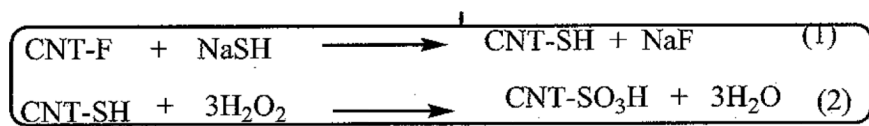


Fig. 5. XPS spectra in the regions of (a) C 1s and (b) S 2p for CNT-F control reaction (in blue and green) overlaid with actual CNT-SH, **1** (purple) and CNT-SO₃H, **2** (black). (For the interpretation of the reference to colour in this figure legend, the reader is referred to the web version of this article.)

**Scheme 1.**